Automated Volumetric Analysis of Interface Fluid in Descemet Stripping Automated Endothelial Keratoplasty Using Intraoperative Optical Coherence Tomography

David Xu,[1,2] William J. Dupps Jr,[2,3] Sunil K. Srivastava,[2] and Justis P. Ehlers[2]

[1]Cleveland Clinic Lerner College of Medicine, Cleveland Clinic, Cleveland, Ohio, United States
[2]Ophthalmic Imaging Center, Cole Eye Institute, Cleveland Clinic, Cleveland, Ohio, United States
[3]Biomedical Engineering, Lerner Research Institute, Cleveland Clinic, Cleveland, Ohio, United States

Correspondence: William J. Dupps Jr, 9500 Euclid Ave/i-32, Cleveland, OH 44195, USA; bjdupps@sbcglobal.net.

Submitted: March 13, 2014
Accepted: July 22, 2014

Citation: Xu D, Dupps WJ Jr, Srivastava SK, Ehlers JP. Automated volumetric analysis of interface fluid in Descemet stripping automated endothelial keratoplasty using intraoperative optical coherence tomography. *Invest Ophthalmol Vis Sci*. 2014;55:5610–5615. DOI:10.1167/iovs.14-14346

Purpose. We demonstrated a novel automated algorithm for segmentation of intraoperative optical coherence tomography (iOCT) imaging of fluid interface gap in Descemet stripping automated endothelial keratoplasty (DSAEK) and evaluated the effect of intraoperative maneuvers to promote graft apposition on interface dimensions.

Methods. A total of 30 eyes of 29 patients from the anterior segment arm of the PIONEER study was included in this analysis. The iOCT scans were entered into an automated algorithm that delineated the spatial extent of the fluid interface gap in three dimensions between donor and host cornea during surgery. The algorithm was validated against manual segmentation, and performance was evaluated by absolute accuracy and intraclass correlation coefficient. Patients underwent DSAEK using a standard sequence of maneuvers, including controlled elevation of IOP and compressive corneal sweep to promote graft adhesion. Measurement of interface fluid volume, en face area, and maximal interface height were compared between scans before anterior chamber infusion, after pressure elevation alone, and after corneal sweep with pressure elevation using dependent-samples *t*-test.

Results. The algorithm achieved 87% absolute accuracy and an intraclass correlation of 0.96. Nine datasets of a total of 84 (11%) required human correction of segmentation errors. Mean interface fluid volume was significantly decreased by corneal sweep ($P = 0.021$) and by both maneuvers combined ($P = 0.046$). Mean en face area was significantly decreased by corneal sweep ($P = 0.010$) and the maneuvers combined ($P < 0.001$). Maximal interface height was significantly decreased by pressure elevation ($P = 0.010$), corneal sweep ($P = 0.009$), and the maneuvers combined ($P = 0.010$).

Conclusions. Quantitative analysis of iOCT volumetric scans shows the significant effect of controlled pressure elevation and corneal sweep on graft apposition in DSAEK. Computerized iOCT analysis yields objective measurements of interface fluid intraoperatively, which provides information on anatomic outcomes and could be used in future trials.

Keywords: optical coherence tomography, endothelial keratoplasty, interface, intraoperative, volume

Corneal transplantation has evolved over the past two decades from conventional penetrating keratoplasty (PK) to selective lamellar transplantation for many conditions.[1,2] Descemet stripping automated endothelial keratoplasty (DSAEK) has supplanted PK as the preferred surgical approach for corneal endothelial dysfunction.[3–5] Compared to PK, DSAEK has the advantage of faster visual recovery, more predictable refractive outcome, a smaller suture burden, minimally invasive repeatability in the event of graft failure, and greater recipient cornea mechanical integrity.[6–11]

The most common early postoperative complication of DSAEK is donor graft dislocation.[12] The reported graft dislocation rate can exceed 25%, particularly in a surgeon's initial experience with the technique.[12,13] Graft dislocation necessitates a repeat operation for repositioning and further manipulation of the graft tissue, and also is associated with increased risk of subsequent graft failure.[14] A variety of techniques have been used to minimize graft dislocation, including short-term air tamponade with passive or controlled pressure elevation, face-up positioning, corneal venting incisions, and compressive corneal sweeping. An important barrier to assessment of the effect of such maneuvers on DSAEK lenticule apposition is the lack of an automated segmentation routine for analyzing interface gap dimensions.

Spectral-domain optical coherence tomography (SD-OCT) is a high-speed, noncontact laser interferometry tool that enables in vivo, tomographic imaging. The use of SD-OCT has significantly impacted the clinical management of a wide range of ophthalmic diseases.[15] More recently, OCT has been adapted for the intrasurgical setting through the use of a portable SD-OCT system, a microscope-mounted portable SD-OCT system, or a microscope integrated system.[16–20] This technology enables high-resolution visualization of tissue effects due to microsurgical manipulations and serves as an adjunct to

microscope visualization of the tissue.[21,22] Pilot studies have demonstrated the feasibility of intraoperative OCT (iOCT) during anterior segment surgery, which visualized the unfolding and positioning of the lamellar graft in DSAEK as well as drainage of interface fluid.[23–25]

When visualized using iOCT, the region of interface fluid is well-bounded anteriorly and posteriorly and has high contrast to the corneal tissue, providing an opportunity for reliable computer segmentation. Such segmentation could address the need for reproducible, quantitative analysis of the interface fluid dimensions as a function of various surgical manipulations thought to promote graft adherence. We previously introduced the use of a graph searching algorithm for the automated assessment of the three dimensional geometry of macular holes in the clinical and intraoperative setting.[26,27] In this report, the authors propose the use of iOCT to evaluate the intrasurgical apposition of the donor graft and host cornea in DSAEK based on the presence of interface fluid using a novel segmentation algorithm.

Methods

Automated Segmentation General Description

A computerized algorithm was developed to reproducibly identify regions of DSAEK interface gap in iOCT data. The general steps in image analysis consist of filtering steps to reduce image noise and applying a curvilinear transformation of the OCT image to flatten the cornea. Next, candidate interface areas within the gross region identified as corneal tissue are selected by searching for the characteristically reduced signal intensity. Candidate areas are identified by searching for small as well as large interface gaps. These candidate areas, thus, describe a general shape and subregion within the image to perform the segmentation. Using a graph searching algorithm, which we have adapted from a previous method for the segmentation of macular holes in macular OCT, we attempted to optimally delineate the boundary between corneal stromal tissue and the fluid interface by examining the local and regional image intensity and gradient. We proceeded with this segmentation through each adjacent OCT cross-section starting from the cross-section that we approximately denoted as the corneal apex—the frame with the greatest mean signal intensity. With the segmentation completed in each frame, we calculated the en face area by projecting the three dimensional segmentation result in the en face plane and the volume by voxel counting. The segmentation results and calculations were reviewed qualitatively by the user for accuracy.

Automated Segmentation Technical Description

Volumetric data from 12×12 mm cube scans with 100 B-scans per volume were extracted in 640×480 pixel resolution. One of every two OCT frames was analyzed to decrease processing time, leading to a sampling density of 1 B-scan every 240 μ. This value was used for interpolation of z-direction value for interpolation of the images.

The major limitations in handheld iOCT imaging compared to clinical table-top scanners are those of image decentration and variable image quality within each cross-section. Variable image quality is a significant limitation to existing segmentation algorithms, which depend on the reliable detection of the anterior and posterior corneal boundaries. Our segmentation goal was to optimally identify the interface fluid gap between donor and recipient cornea even in the face of inconsistent image quality.

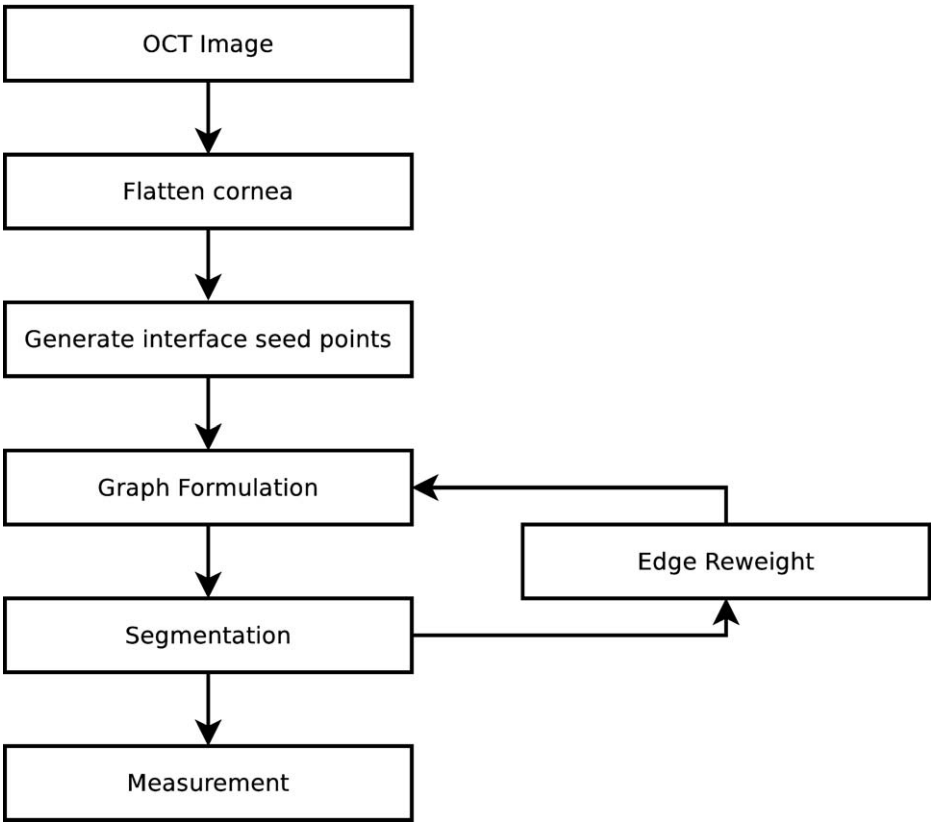

Figure 1. Schematic diagram of the segmentation algorithm.

Investigative Ophthalmology & Visual Science

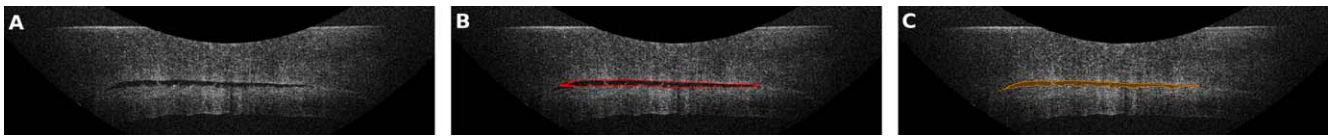

FIGURE 2. (**A**) iOCT cross-section of eye undergoing Descemet stripping automated endothelial keratoplasty. The scan is first dewarped to bring the cornea into a horizontal position. (**B**) Seed points are identified in coarse and fine grids. (**C**) The final segmentation is produced by the method of graph cuts.

The segmentation algorithm proceeded in four general steps consisting of preprocessing, identification of interface seed points, segmentation using graph search, and volume calculation (Fig. 1). Segmentation was performed on a frame-by-frame basis with the adjacent frame's segmentation result serving as a priori input for the current segmentation. First, every frame was filtered with a 10×10 pixel Gaussian averaging filter to reduce noise. The region to be classified grossly as cornea was identified by intensity thresholding followed by removal of small islands and discontinuous regions using morphological filtering. Next, the image was warped in the axial direction such that the corneal region achieved a flat shape horizontally (Fig. 2A). Each A-scan in the cross-section was transposed vertically by an offset, which was determined from the fitting of a curvilinear spline to the point of greatest signal intensity. This warped the cornea to the degree such that the region of the cornea was grossly flat. Image warping was performed because it reduced the rectangular region of interest that encompassed the interface fluid, improving algorithm performance. Our algorithm specifically does not perform direct segmentation of the anterior and posterior corneal boundaries, and, thus, avoids a major source of segmentation failure.

Seed pixels in regions known to be interface fluid (foreground) were identified in a multi-scale search based on image intensity. A coarse seed map was created by intensity thresholding of the difference map between the flattened OCT image and the same image morphologically closed by a rectangular structuring element. Because of noise adjacent to the anterior and posterior corneal surface, seed points were eliminated if they fell on the edge of the corneal region. Next, a fine seed map was created by intensity thresholding of a difference map generated using a small structuring element (Fig. 2B). Regions in the fine seed map were retained only of they fell within the extent of the coarse seed map.

The final segmentation was performed using graph cuts implemented in a similar fashion to our previous report for which a more formal mathematical is provided.[26] In brief, we used an undirected graph with vertices representing image pixels in an 8-connected neighborhood system. Edges between neighbors encode local image gradient. Pixel intensity is encoded by edge weight between each vertex to two special vertices, the sink and the source. The minimum cut optimally bipartitions the graph into two unconnected subgraphs, the foreground and the background, representing the regions of interface fluid and the adjacent cornea. The resulting segmentation minimizes the aggregate boundary cost of summed image gradients and the summed intensity of the segmented region. This implementation produced robust results even in the presence of significant noise and image variability (Fig. 2C).

Segmentation started from the frame with the greatest mean image intensity to approximate the location of the corneal apex. Adjacent frames subsequently were processed. Results from the previous frame were used to reweight edges in the current graph to favor a segmentation of similar shape and location to the previous result. The segmentation from individual frames was assembled to calculate total interface fluid volume and en face area of interface gap. Volumetric calculation was performed by counting voxels inscribed in the surface. Calculation of en face area was performed by axial projection of the segmentation result to a two-dimensional plane and counting pixels with fluid. The maximal interface gap height was calculated as the maximal axial height of the fluid in any cross-section. The algorithm was implemented in MATLAB (Mathworks, Inc., Natick, MA, USA) and the graph search was implemented in C++ (GNU Compiler Collection; Free Software Foundation, Inc., Boston, MA, USA). The human operator qualitatively reviews the OCT dataset and the frame-by-frame segmentations to verify plausible results. If refinement is necessary, manual selection of the boundary can be performed and the subsequent frames rerun to incorporate the full range of a priori results.

Patients and Image Acquisition

The analysis included consecutive patients undergoing DSAEK from February 2012 to August 2012 for corneal endothelial dystrophy or corneal edema due to endothelial failure who were enrolled in the PIONEER study, a prospective, single-center study examining the use of intraoperative and perioperative OCT in ophthalmic surgery. A single surgeon

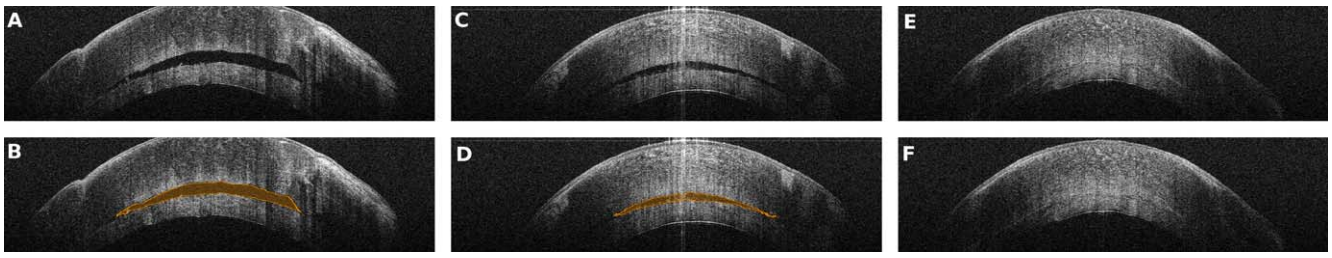

FIGURE 3. SD-OCT cross-sections and segmentation results in the same eye in a 74-year-old patient undergoing DSAEK for failed prior PK immediately after delivery and unfolding of the donor graft (**A**, **B**). After elevation of the intraocular pressure, the size of the gap is decreased (**C**, **D**). After sweeping maneuver, there is no interface gap (**E**, **F**).

Table 1. Mean Interface Fluid Volume, En Face Area, and Maximal Interface Height in iOCT Imaging After Delivery and Unfolding of the Graft, After Pressure Elevation, and After Corneal Sweep

	Volume, mm^3 (Range)	En Face Area, mm^2 (Range)	Interface Height, μm (Range)
After unfolding	0.452 ± 1.12 (0–5.71)	4.17 ± 5.03 (0–19.2)	125 ± 147 (0–795)
After pressure elevation	0.070 ± 0.126 (0–0.458)	1.31 ± 1.94 (0–7.03)	80.2 ± 61.6 (0–276)
After corneal sweep	0.011 ± 0.023 (0–0.111)	0.28 ± 0.613 (0–3.29)	48.8 ± 35.8 (0–137)

(WJD) performed the surgery for all patients in the cohort included in this report using a standardized sequence of maneuvers. All cases incorporated the use of an initial manual injection of air delivered with a bent 30-gauge needle used to simultaneously pinion the periphery of the graft against the recipient stroma, control elevation of the anterior chamber pressure for short time periods, and perform compressive corneal sweep maneuvers during active anterior chamber infusion to promote graft adherence.[28–31] No corneal venting incisions were created. Imaging was performed according to the PIONEER DSAEK scan protocol using a customized microscope-mounted iOCT system that used the Bioptigen SDOIS system (Bioptigen, Inc., Research Triangle Park, NC, USA). Raster scans were acquired in 12 × 12 mm cube scans with 100 B-scans per volume. Each eye underwent iOCT imaging at three time points: after unfolding of the graft and noncontinuous insufflation of air in the anterior chamber, after elevation of the anterior chamber pressure for a short time period with active infusion (Accurus Vitreoretinal Surgical System; Alcon, Fort Worth, TX, USA), and after corneal sweep with a flat irrigation cannula on a balanced salt solution squeeze bottle. The study was approved by the Institutional Review Board of the Cleveland Clinic and adhered to the tenets of the Declaration of Helsinki. All patients provided informed consent for enrollment in the PIONEER study.

Validation and Analysis

Validation of the algorithm was performed by comparison of the segmentation results to a human grader in an OCT frame at the corneal apex from the first 20 consecutive cases. The interface gap boundary was delineated manually by a masked human grader (DX) and cross-sectional area was calculated by pixel counting in the human and computer segmentations. Absolute accuracy was defined as the difference between the human and computer cross-sectional area divided by the human result. Absolute accuracy and intraclass correlation of the square root of the cross-sectional area were used to assess algorithmic performance against this standard. After algorithm validation, volumetric analysis of the iOCT datasets was performed for all eyes. Interface volume, en face area, and maximal gap height were compared between scans at the three operative time points using dependent-samples *t*-test with significance criteria of $P < 0.05$. The proportion of eyes that had a fluid volume greater than 0.1 mm^3 after pressure elevation and after corneal sweep was compared by McNemar's test.

Results

Validation

An initial set of 20 consecutive cases were analyzed and compared to a masked grader. The algorithm achieved 87% absolute accuracy compared to the human grader. The intraclass correlation was 0.96. Volumetric analysis was performed successfully in all patients and time points. The OCT segmentations were reviewed qualitatively by a human grader and invalid segmentations were identified manually. Of the 84 datasets (three time points each from 28 eyes), nine required manual correction (11%).

Intrasurgical Analysis

We included in this analysis 30 eyes of 29 patients undergoing DSAEK from the PIONEER study. Two cases did not have iOCT scanning at all three time points and were excluded. The remaining 28 eyes of 27 patients (14 left, 14 right) underwent DSAEK for Fuchs endothelial dystrophy (14 eyes), pseudophakic bullous keratopathy (9 eyes), endothelial failure after prior DSAEK (2 eyes), and endothelial failure after prior PK (3 eyes). The mean age was 73 ± 15 years. The mean baseline best corrected Snellen visual acuity (BCVA) was 20/190. The mean 6-month postoperative BCVA was 20/40 ($P = 0.003$). Graft dislocation occurred in one eye with prior PK on postoperative day 1 and underwent repeat endothelial keratoplasty.

Intraoperative imaging was performed in all eyes after unfolding of the graft by instillation of an air bubble, after brief elevation of the anterior chamber pressure, and after corneal sweep. Volumetric analysis was performed successfully in post hoc processing for all eyes and time points, and nine datasets produced invalid results that required human correction (Fig. 3). Mean interface fluid volume, en face area, and maximal interface fluid height were calculated from each scan (Table 1). One of 28 eyes had no detectable fluid immediately after graft delivery, while three of 28 eyes had no detectable interface fluid after corneal sweep. The variation in interface fluid volume was greatest after delivery of the graft without flattening maneuvers, ranging from no fluid identified to 5.71 mm^3. A total of 13 eyes had an interface fluid volume greater than 0.1 mm^3 immediately after delivery of the graft, compared to 6 eyes after pressure elevation ($P = 0.081$), and 1 eye after corneal sweep ($P < 0.001$). Interface fluid volume was decreased significantly after corneal sweep ($P = 0.021$) and

Table 2. Change in Total Interface Gap Volume, En Face Area, and Maximal Interface Height After Controlled Pressure Elevation, After Corneal Sweeping, and After the Maneuvers Combined

	After Unfolding to After Pressure Elevation (*P* Value)	After Pressure Elevation to After Corneal Sweep (*P* Value)	After Unfolding to After Corneal Sweep (*P* Value)
Volume change, mm^3	−0.382 (0.080)	−0.059 (0.021)	−0.441 (0.046)
En face area change, mm^2	−2.86 (0.119)	−1.03 (0.010)	−3.89 (<0.001)
Interface height change, μm	−45.3 (0.001)	−31.4 (0.009)	−76.7 (0.010)

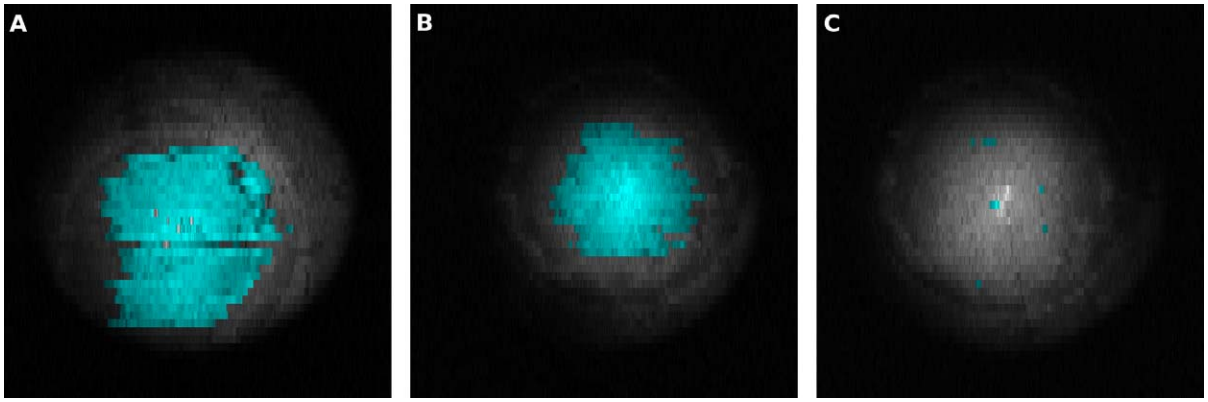

FIGURE 4. False color map of en face fluid in the same patient as Figure 3 after delivery of the graft (**A**), pressure elevation (**B**), and after sweep (**C**). The intensity of the color signifies the height of the fluid at that location.

after the pressure elevation and corneal sweep steps ($P = 0.046$). En face area also was significantly decreased by corneal sweep ($P = 0.010$) and serial pressure elevation and corneal sweep ($P < 0.001$). The maximal interface fluid height was decreased significantly by pressure elevation alone ($P = 0.001$), corneal sweep ($P = 0.009$), and both maneuvers in series ($P = 0.010$, Table 2). The postcorneal sweep volume, en face area, and height in the eye with subsequent graft dehiscence were below the median value of the cohort, although the post-insertion and postpressure elevation volume, area, and height were above the 75th percentile (Fig. 4).

DISCUSSION

In this study, an automated graph searching approach was used to delineate the spatial extent of interface fluid gap between DSAEK donor and host cornea in iOCT. To our knowledge, this is the first study to analyze quantitatively intraoperative imaging in three dimensions in the anterior segment. As the first study evaluating the methodology, we successfully applied the analysis to a consecutive series of patients undergoing DSAEK for a range of pathology, including Fuchs' dystrophy, pseudophakic bullous keratopathy, and patients with failed prior PK and endothelial keratoplasty. Currently, the standard for evaluation of DSAEK graft stability is the en face view through the surgical microscope. The iOCT provides the surgeon with extensive anatomic cross-sectional information. While qualitative evaluation of iOCT cross-sections may be used to guide surgical decision-making during DSAEK, the manual evaluation of the scans could be limited by variability between different observers and the time it takes to review the relatively large volume of data collected. A computerized method that achieves reproducible three-dimensional analyses to a degree suitable for clinical use in OCT scans with variable signal strength and centration could provide an important objective measure of the fluid interface. In addition, we introduce the computer measurement of the en face area of interface fluid. This "fluid map" identifies the location of the fluid in an automated fashion and may help to direct surgeons to the pertinent location for additional surgical manipulations.

To explore the utility of the analysis further, we analyzed intraoperative datasets at three time points in DSAEK surgery as techniques were used to promote donor graft adhesion: after delivery and unfolding of the graft, after controlled spikes in pressure, and after compressive corneal sweep at elevated pressure. The analysis demonstrates statistically significant decreases in the in vivo volume, en face area, and maximal height of the interface fluid. These findings are in agreement with qualitative findings based on examination of iOCT cross-sectional images and experiments using an artificial anterior chamber.[23,24,32]

The presence of an interface gap is frequently seen in DSAEK surgery, and it generally is believed that fluid in the interface may predispose to detachment of the graft. The resolution of fluid is thought to be related to endothelial pump function and persistent gas tamponade applying pressure to the lamellar graft. However, the relationship between intraoperative interface fluid and graft dislocation has not been the subject of comparative studies. In our review of the literature, we were unable to identify other studies that quantified the interface fluid associated with graft dislocation. This study serves as a foundation for future research regarding the relationship of interface fluid and its potential association with surgical outcomes. Additionally, this tool may provide a unique opportunity in clinical trials for objectively assessing interface fluid intraoperatively.

The findings of this study are the result of an automated segmentation method that reduces subjectivity, and has accuracy and intraclass correlation suitable for clinical use. However, there are several limitations of the study. Portable intraoperative SD-OCT imaging often yields lower image quality than bench-top scanners, and this was the principle limitation in accurate segmentation in both human graders and computer analysis. A review of the segmentation results demonstrated that most of the variability between human and computer segmentation was in regions with lower image quality. We made no attempts to extrapolate segmentation results in the region overlapping the central corneal reflection artifact. This leads to a systematic negative bias in the calculation of volume. However, in some eyes, fluid was present in discontinuous pockets and we felt it was not appropriate to extrapolate between these regions. Finally, failure of the segmentation algorithm requiring human intervention occurs in images with complex morphology and poorer signal-to-noise ratio. This is a significant limitation which further optimization of the algorithm would lessen, but not completely eliminate.

In conclusion, we present a novel computerized segmentation algorithm to analyze the interface fluid volume and area in iOCT of DSAEK surgery. We found a significant decrease in interface fluid volume with serial anterior chamber pressurization and compressive corneal maneuvers. Future planned areas of research include prospective quantitative assessment of interface fluid to better delineate the role of fluid in surgical outcomes.

Acknowledgments

Supported by National Institutes of Health (Bethesda, MD, USA) Grants NIH/NEI K23-EY022947-01A1 (JPE) and NIH/NEI R01 EY023381 (WJD), and Ohio Department of Development TECH-13-059 (JPE, WJD, SKS). The authors alone are responsible for the content and writing of the paper.

Disclosure: **D. Xu**, None; **W.J. Dupps Jr**, Avedro (F), Zeiss (F), Ziemer Ophthalmic Systems (C); **S.K. Srivastava**, Allergan (F), Leica (C), Bausch and Lomb (C), P; **J.P. Ehlers**, Thrombogenics (C, R), Zeiss (C), Leica (C), P

References

1. Melles GR, Eggink FA, Lander F, et al. A surgical technique for posterior lamellar keratoplasty. *Cornea*. 1998;17:618–626.
2. Terry MA. A new approach for endothelial transplantation: deep lamellar endothelial keratoplasty. *Int Ophthalmol Clin*. 2003;43:183–193.
3. Melles GRJ, Lander F, Nieuwendaal C. Sutureless, posterior lamellar keratoplasty: a case report of a modified technique. *Cornea*. 2002;21:325–327.
4. Price MO, Price FW Jr. Descemet's stripping with endothelial keratoplasty: comparative outcomes with microkeratome-dissected and manually dissected donor tissue. *Ophthalmology*. 2006;113:1936–1942.
5. Gorovoy MS. Descemet-stripping automated endothelial keratoplasty. *Cornea*. 2006;25:886–889.
6. Jun B, Kuo AN, Afshari NA, Carlson AN, Kim T. Refractive change after descemet stripping automated endothelial keratoplasty surgery and its correlation with graft thickness and diameter. *Cornea*. 2009;28:19–23.
7. Lee WB, Jacobs DS, Musch DC, Kaufman SC, Reinhart WJ, Shtein RM. Descemet's stripping endothelial keratoplasty: safety and outcomes: a report by the American Academy of Ophthalmology. *Ophthalmology*. 2009;116:1818–1830.
8. Price FW Jr, Price MO. Descemet's stripping with endothelial keratoplasty in 200 eyes: Early challenges and techniques to enhance donor adherence. *J Cataract Refract Surg*. 2006;32:411–418.
9. Gorovoy MS, Meisler DM, Dupps WJ Jr. Late repeat Descemet-stripping automated endothelial keratoplasty. *Cornea*. 2008;27:238–240.
10. Ratanasit A, Gorovoy MS. Long-term results of Descemet stripping automated endothelial keratoplasty. *Cornea*. 2011;30:1414–1418.
11. Titiyal JS, Sachdev R, Sinha R, Tandon R, Sharma N. Modified surgical technique for improving donor adherence in DSAEK in the aphakic vitrectomized eye. *Cornea*. 2012;31:462–464.
12. Suh LH, Yoo SH, Deobhakta A, et al. Complications of Descemet's stripping with automated endothelial keratoplasty: survey of 118 eyes at One Institute. *Ophthalmology*. 2008;115:1517–1524.
13. Koenig SB, Covert DJ, Dupps WJ Jr, Meisler DM. Visual acuity, refractive error, and endothelial cell density six months after Descemet stripping and automated endothelial keratoplasty (DSAEK). *Cornea*. 2007;26:670–674.
14. O'Brien PD, Lake DB, Saw VP, Rostron CK, Dart JK, Allan BD. Endothelial keratoplasty: case selection in the learning curve. *Cornea*. 2008;27:1114–1118.
15. Chen TC, Cense B, Pierce MC, et al. Spectral domain optical coherence tomography: ultra-high speed, ultra-high resolution ophthalmic imaging. *Arch Ophthalmol*. 2005;123:1715–1720.
16. Dayani PN, Maldonado R, Farsiu S, Toth CA. Intraoperative use of handheld spectral domain optical coherence tomography imaging in macular surgery. *Retina*. 2009;29:1457–1468.
17. Ray R, Barañano DE, Fortun JA, et al. Intraoperative microscope-mounted spectral domain optical coherence tomography for evaluation of retinal anatomy during macular surgery. *Ophthalmology*. 2011;118:2212–2217.
18. Ehlers JP, Tao YK, Farsiu S, Maldonado R, Izatt JA, Toth CA. Visualization of real-time intraoperative maneuvers with a microscope-mounted spectral domain optical coherence tomography system. *Retina*. 2013;33:232–236.
19. Ehlers JP, Gupta PK, Farsiu S, et al. Evaluation of contrast agents for enhanced visualization in optical coherence tomography. *Invest Ophthalmol Vis Sci*. 2010;51:6614–6619.
20. Binder S, Falkner-Radler CI, Hauger C, Matz H, Glittenberg C. Feasibility of intrasurgical spectral-domain optical coherence tomography. *Retina*. 2011;31:1332–1336.
21. Ehlers JP, Kernstine K, Farsiu S, Sarin N, Maldonado R, Toth CA. Analysis of pars plana vitrectomy for optic pit-related maculopathy with intraoperative optical coherence tomography: a possible connection with the vitreous cavity. *Arch Ophthalmol*. 2011;129:1483–1486.
22. Ehlers JP, Tao YK, Farsiu S, Maldonado R, Izatt JA, Toth CA. Integration of a spectral domain optical coherence tomography system into a surgical microscope for intraoperative imaging. *Invest Ophthalmol Vis Sci*. 2011;52:3153–3159.
23. Knecht PB, Kaufmann C, Menke MN, Watson SL, Bosch MM. Use of intraoperative fourier-domain anterior segment optical coherence tomography during descemet stripping endothelial keratoplasty. *Am J Ophthalmol*. 2010;150:360–365.
24. Ide T, Wang J, Tao A, et al. Intraoperative use of three-dimensional spectral-domain optical coherence tomography. *Ophthalmic Surg Lasers Imaging*. 2010;41:250–254.
25. Steven P, Le Blanc C, Velten K, et al. Optimizing descemet membrane endothelial keratoplasty using intraoperative optical coherence tomography. *JAMA Ophthalmol*. 2013;131:1135–1142.
26. Xu D, Yuan A, Kaiser PK, et al. A novel segmentation algorithm for volumetric analysis of macular hole boundaries identified with optical coherence tomography. *Invest Ophthalmol Vis Sci*. 2013;54:163–169.
27. Ehlers JP, Xu D, Kaiser PK, Singh RP, Srivastava SK. Intrasurgical dynamics of macular hole surgery: an assessment of surgery-induced ultrastructural alterations with intraoperative optical coherence tomography. *Retina*. 2014;34:213–221.
28. Koenig SB, Dupps WJ Jr, Covert DJ, Meisler DM. Simple technique to unfold the donor corneal lenticule during Descemet's stripping and automated endothelial keratoplasty. *J Cataract Refract Surg*. 2007;33:189–190.
29. Meisler DM, Dupps WJ Jr, Covert DJ, Koenig SB. Use of an air-fluid exchange system to promote graft adhesion during Descemet's stripping automated endothelial keratoplasty. *J Cataract Refract Surg*. 2007;33:770–772.
30. Koenig SB, Meisler DM, Dupps WJ, Rubenstein JB, Kumar R. External refinement of the donor lenticule position during descemet's stripping and automated endothelial keratoplasty. *Ophthalmic Surg Lasers Imaging*. 2008;39:522–523.
31. Price MO, Price FW. Descemet's stripping endothelial keratoplasty. *Curr Opin Ophthalmol*. 2007;18:290–294.
32. Bhogal MS, Angunawela RI, Bilotti E, Eames I, Allan BD. Theoretical, experimental, and optical coherence tomography (OCT) studies of graft apposition and adhesion in Descemets stripping automated endothelial keratoplasty (DSAEK). *Invest Ophthalmol Vis Sci*. 2012;53:3839–3846.

Investigative Ophthalmology & Visual Science